PNAS

Supporting Information for

Activity-Induced MeCP2 Phosphorylation Regulates Retinogeniculate Synapse Refinement

Christopher P. Tzeng[a,1,2], Tess Whitwam[a,1], Lisa D. Boxer[a,1,3], Emmy Li[a], Andrew Silberfeld[a], Sara Trowbridge[a], Kevin Mei[a], Cindy Lin[a], Rebecca Shamah[a], Eric C. Griffith[a], William Renthal[a,4], Chinfei Chen[b,5], Michael E. Greenberg[a,5]

[a]Department of Neurobiology, Harvard Medical School, Boston, MA 02115
[b]Department of Neurology, F.M. Kirby Neurobiology Center, Children's Hospital, Boston, MA 02115

[1]C.P.T, T.W., and L.D.B. contributed equally to this work.
[2]Present address: Department of Biology, Stanford University, Stanford, CA 94305
[3]Present address: Laboratory of Genome Integrity, National Cancer Institute, Bethesda, MD 20892
[4]Present address: Department of Neurology, Brigham and Women's Hospital, Boston, MA 02115
[5]To whom correspondence may be addressed.
Email: Chinfei.Chen@childrens.harvard.edu or Michael_Greenberg@hms.harvard.edu

This PDF file includes:

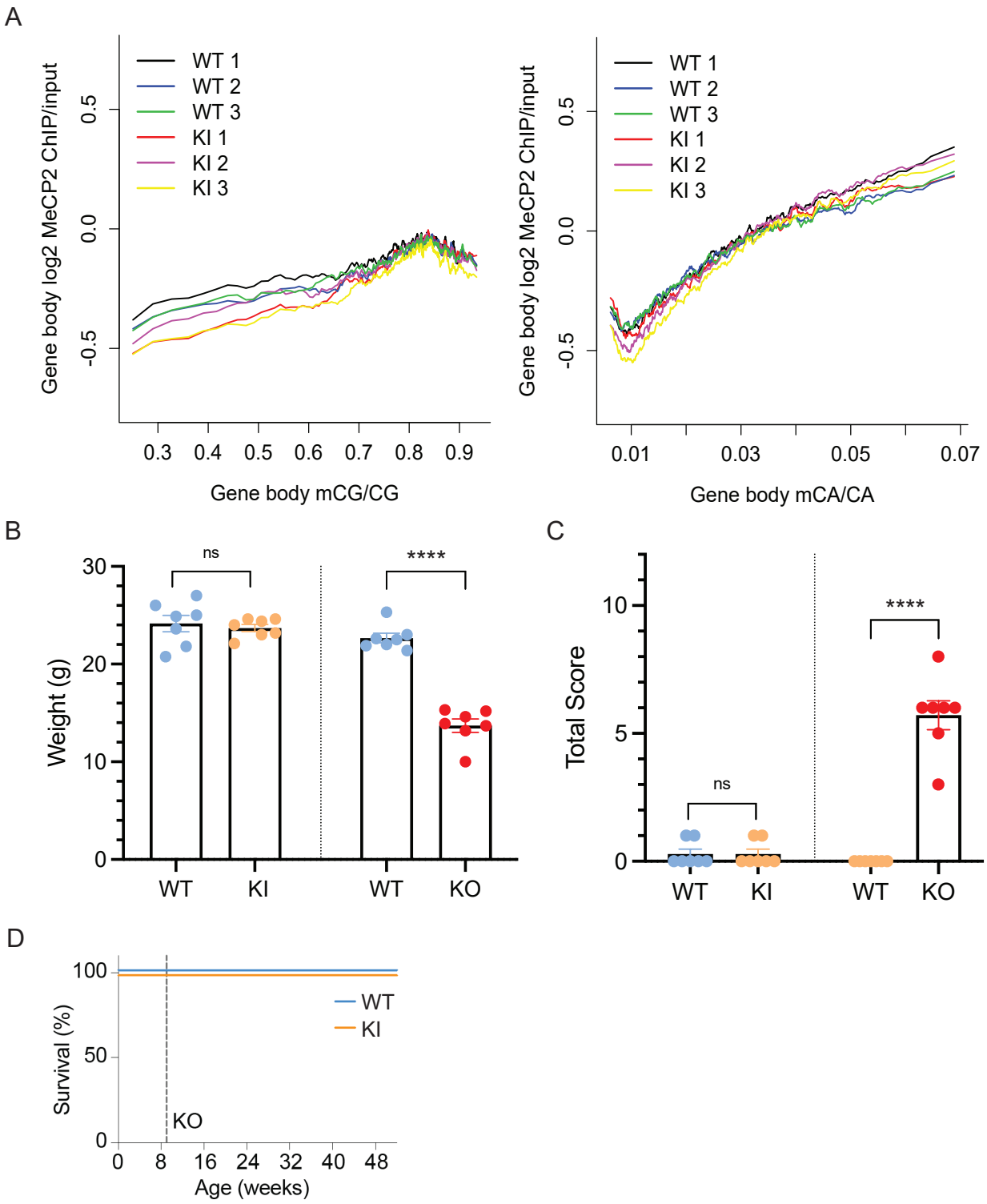

Figure S1. Validation of quadruple knock-in (QKI) mice.
A) MeCP2 exhibits similar binding to methylated DNA in QKI and WT mice. mCG (*Left*) and mCA (*Right*).
B) QKI mice show no differences in weight as compared to WT littermates (n=7). Male littermates were weighed between 6 and 9 weeks of age. Statistics were performed with an unpaired, two-sided, parametric t-test. ns, $p > 0.05$.
C) QKI mice show no differences in Rett Syndrome-like phenotypes, as assessed using a previously established method (Supp Ref. 1). Male littermates were assessed between the ages of 6 and 9 weeks of age (n=7). Statistics were performed with an unpaired, one-sided, parametric t-test. ns, $p > 0.05$; ****, $p < 0.0001$.
D) QKI mice show no differences in longevity as compared to WT littermates. Dashed line indicates typical lifespan of MeCP2 KO mice (Supp Ref. 2). n = 10 WT, 12 QKI.

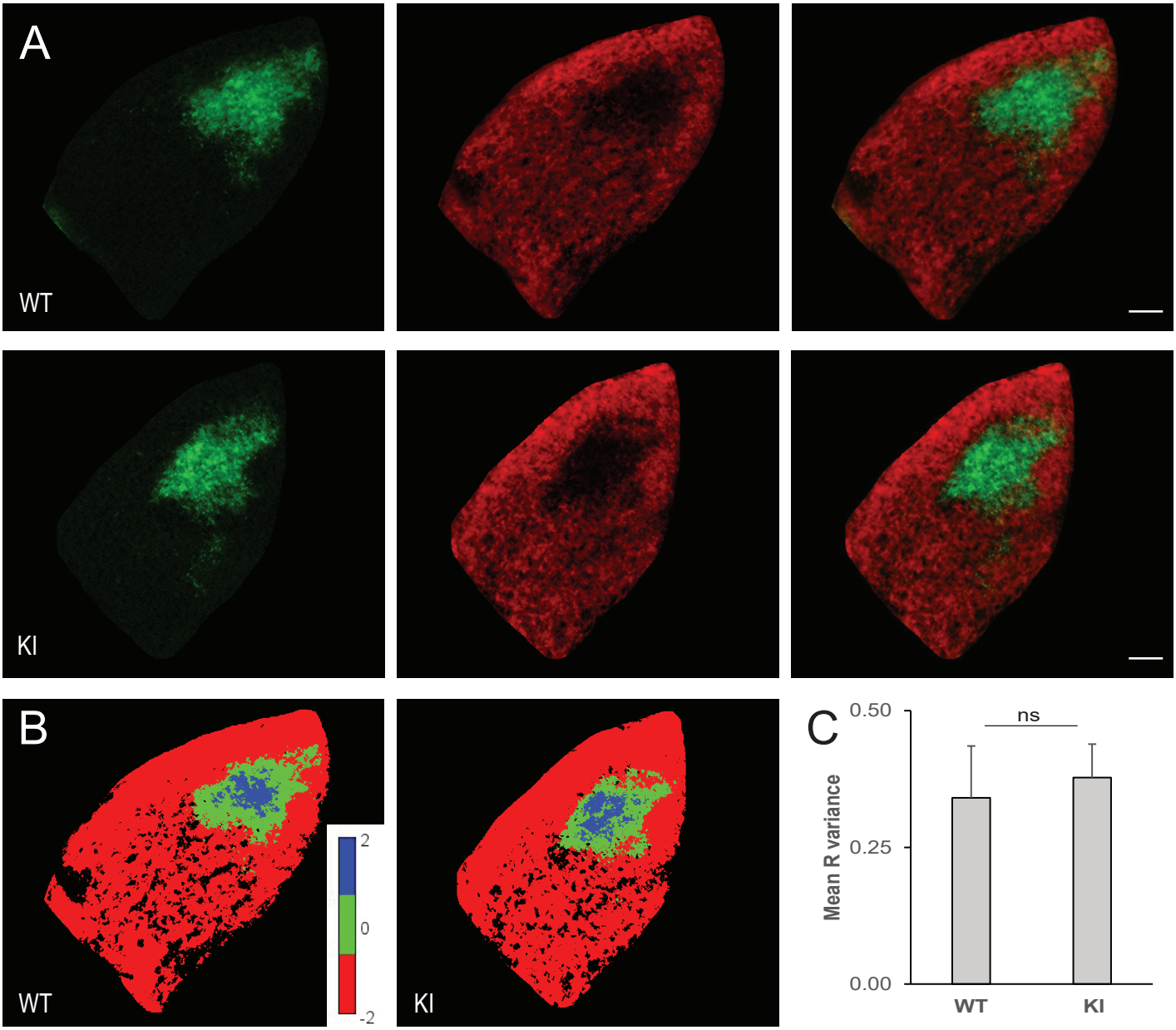

Figure S2. Eye-specific segregation is normal in QKI adult animals.
A) Representative images of coronal sections of the LGN from P58-P64 QKI (*Bottom*) and littermate WT control mice (*Top*) with labeled retinal projections from the ipsilateral eye (green) and contralateral eye (red).
B) Representative images pseudocolored based on R-values, in which ipsilateral-dominated pixels are blue and contralateral-dominated pixels are red.
C) Mean R-variance is not significantly different between WT and QKI mice (p=0.20, two-tailed student t-test). n=16 sections from 4 animals for each genotype. Scale bar = 100 μm. Error bars = standard deviation.

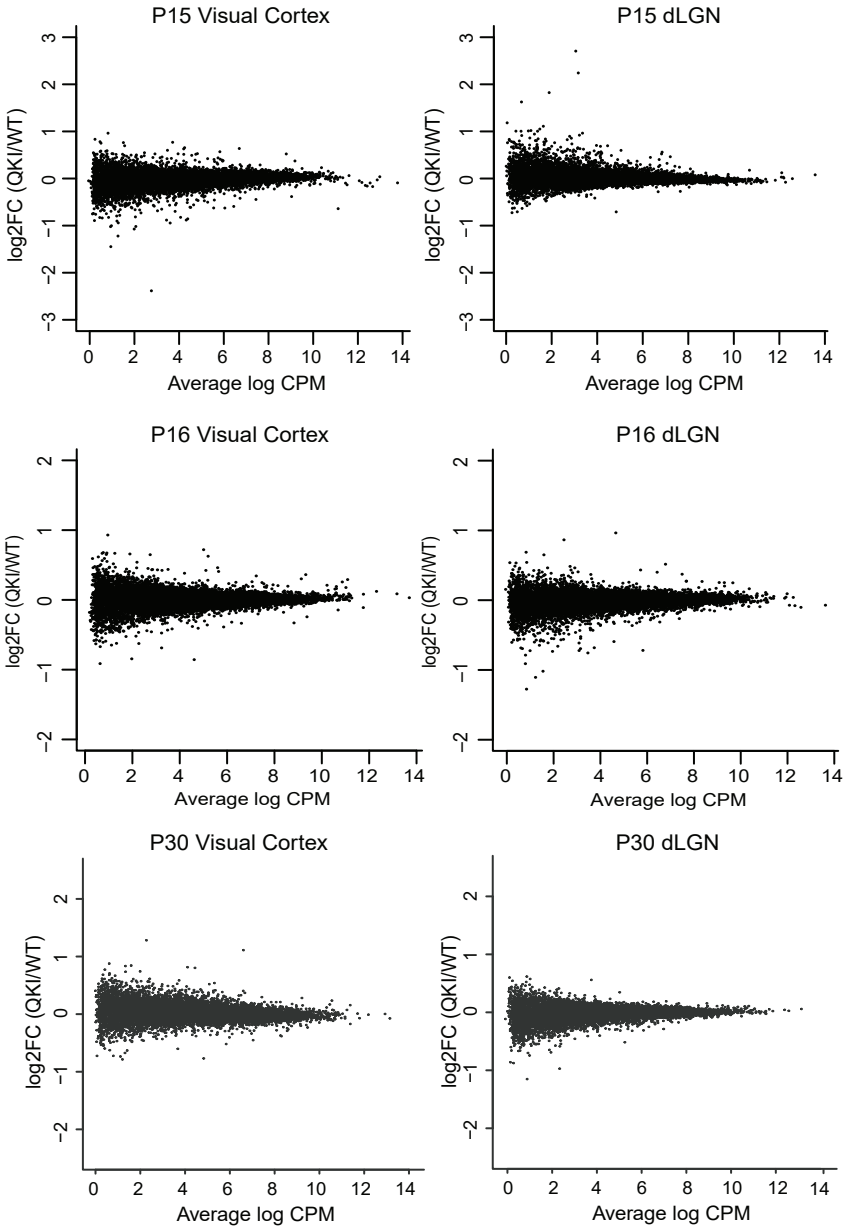

Figure S3. Gene expression analysis in QKI mice.
Mean-difference plots of differential gene expression analysis from bulk RNA-sequencing of 6 WT and 6 QKI visual cortex (*Left*) and dLGN (*Right*) at P15 (*Top*), 10 WT and 10 QKI visual cortex (*Left*) and dLGN (*Right*) at P16 (*Middle*), and 6 WT and 6 QKI visual cortex (*Left*) and dLGN (*Right*) at P30-31 (*Bottom*). No significant differentially expressed genes were detected. Differentially expressed genes were defined by an FDR < 0.05 with no fold-change cut-off. Fisher's exact test with Benjamini-Hochberg correction.

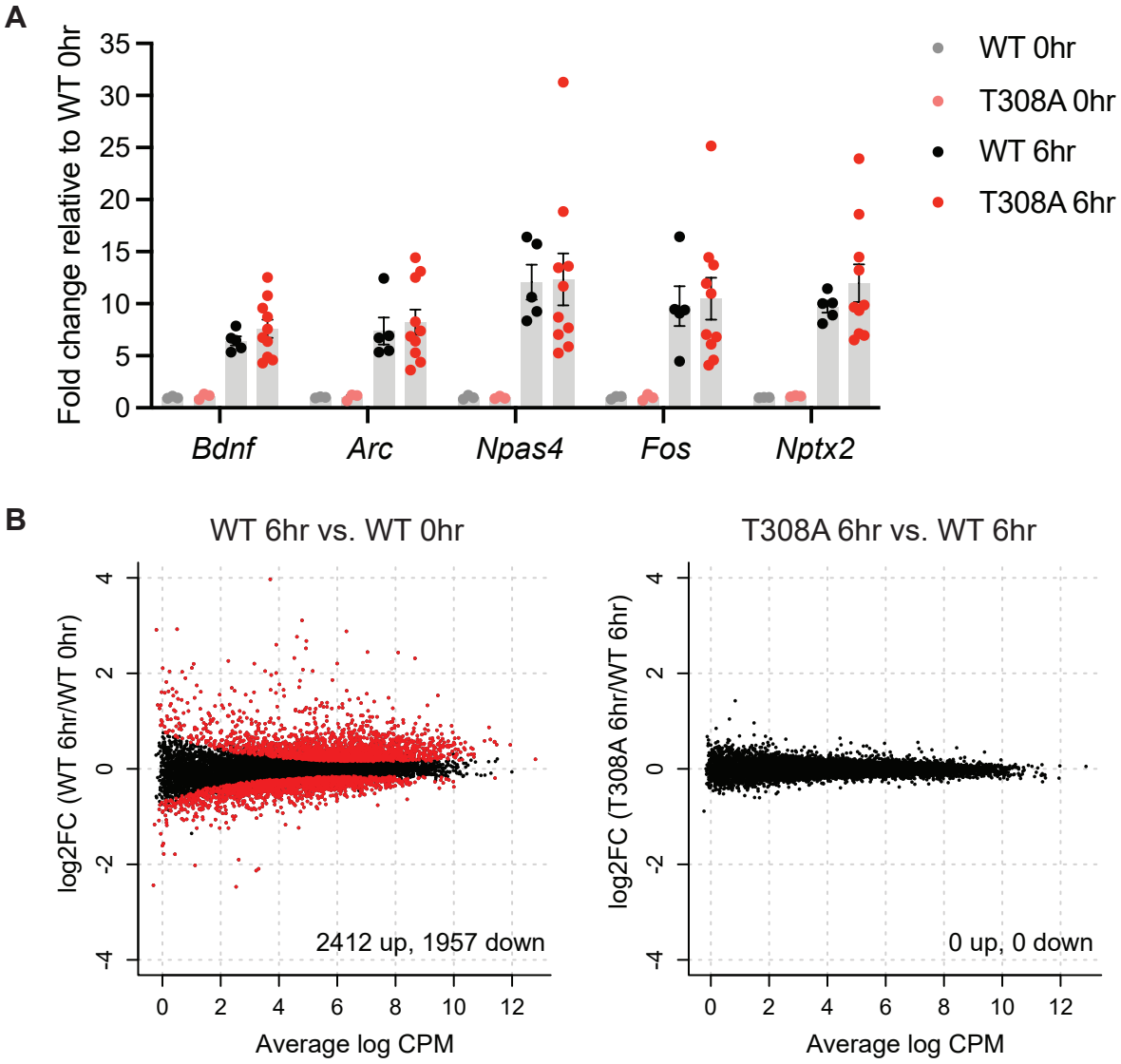

Figure S4. Gene expression analysis of visual cortex from WT and MeCP2 T308A mice.
A) qPCR analysis of activity-induced genes in the visual cortex of 8-week old WT and MeCP2 T308A mice that were dark reared during 6 to 8 weeks of age, then exposed to light for 0 or 6 hours. Fold-change relative to average WT 0 hour is shown. None of the genes are significantly different between WT and T308A mice 6 hours after light exposure (two-tailed unpaired t-test). All individual data points are shown. Bar indicates mean and error bars indicate S.E.M.
B) Mean-difference plots of differential gene expression analysis from RNA-seq of visual cortex from 8-week old WT and MeCP2 T308A mice that were dark reared during 6 to 8 weeks of age, then exposed to light for 0 or 6 hours. Differentially expressed genes shown in red were defined by an FDR < 0.05 with no fold-change cut-off. *Left*: There are 4,369 differentially expressed genes between WT 6hr and WT 0hr. *Right*: There are 0 differentially expressed genes between T308A 6hr and WT 6hr.

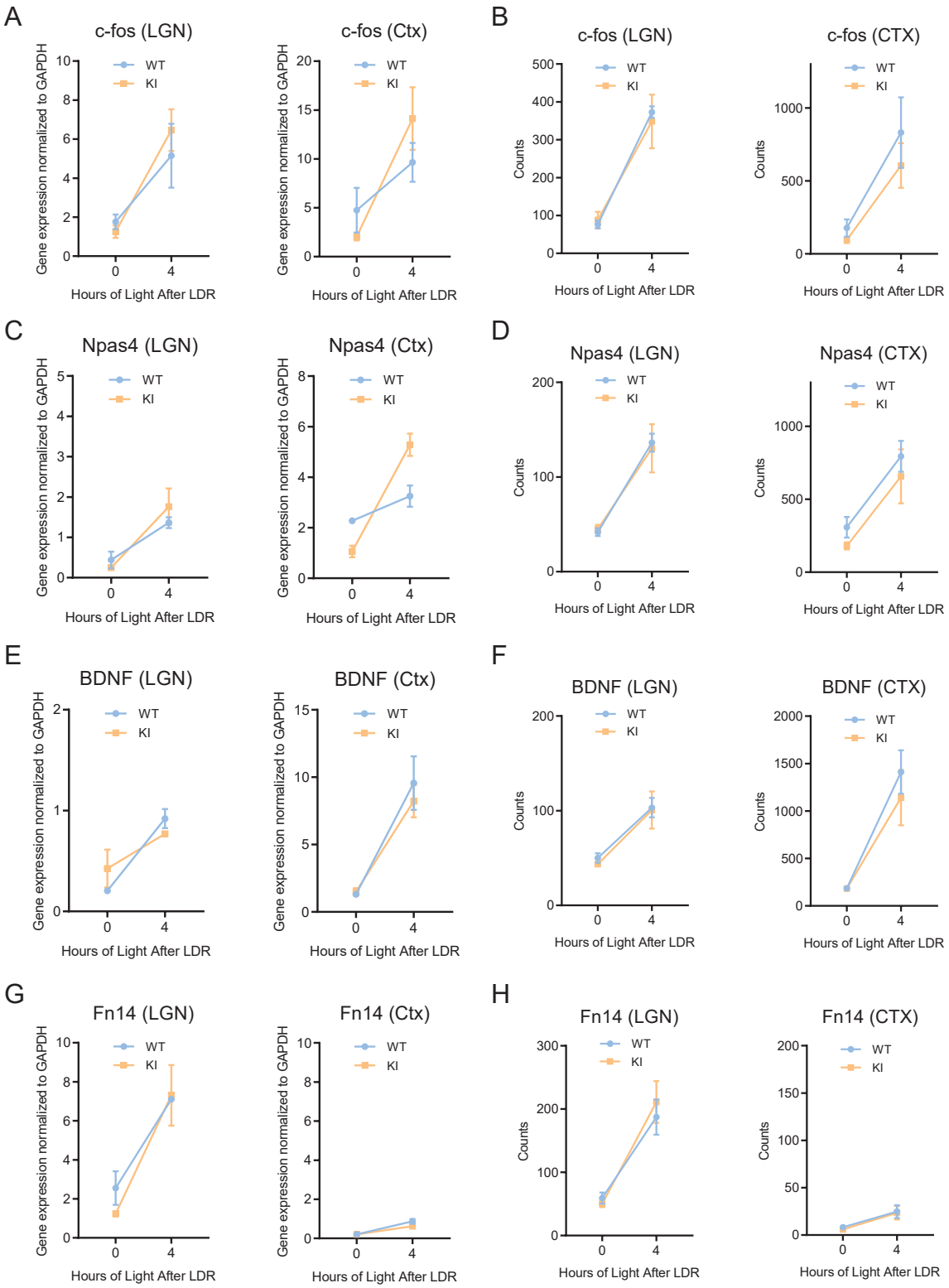

Figure S5. **Validation of late dark rearing (LDR) and light exposure paradigm.**
A-B) Induction of *Fos* in dLGN (*Left*) and visual cortex (*Right*) following LDR and 4 hours of light exposure by RT-qPCR (*A*) and by bulk RNA-Seq (*B*).
C-D) Induction of *Npas4* in dLGN (*Left*) and visual cortex (*Right*) following LDR and 4 hours of light exposure by RT-qPCR (*C*) and by bulk RNA-Seq (*D*).
E-F) Induction of *Bdnf* in dLGN (*Left*) and visual cortex (*Right*) following LDR and 4 hours of light exposure by RT-qPCR (*E*) and by bulk RNA-Seq (*F*).
G-H) Induction of *Tnfrsf12a* (*Fn14*) in dLGN (*Left*) and visual cortex (*Right*) following LDR and 4 hours of light exposure by RT-qPCR (*G*) and by bulk RNA-Seq (*H*).

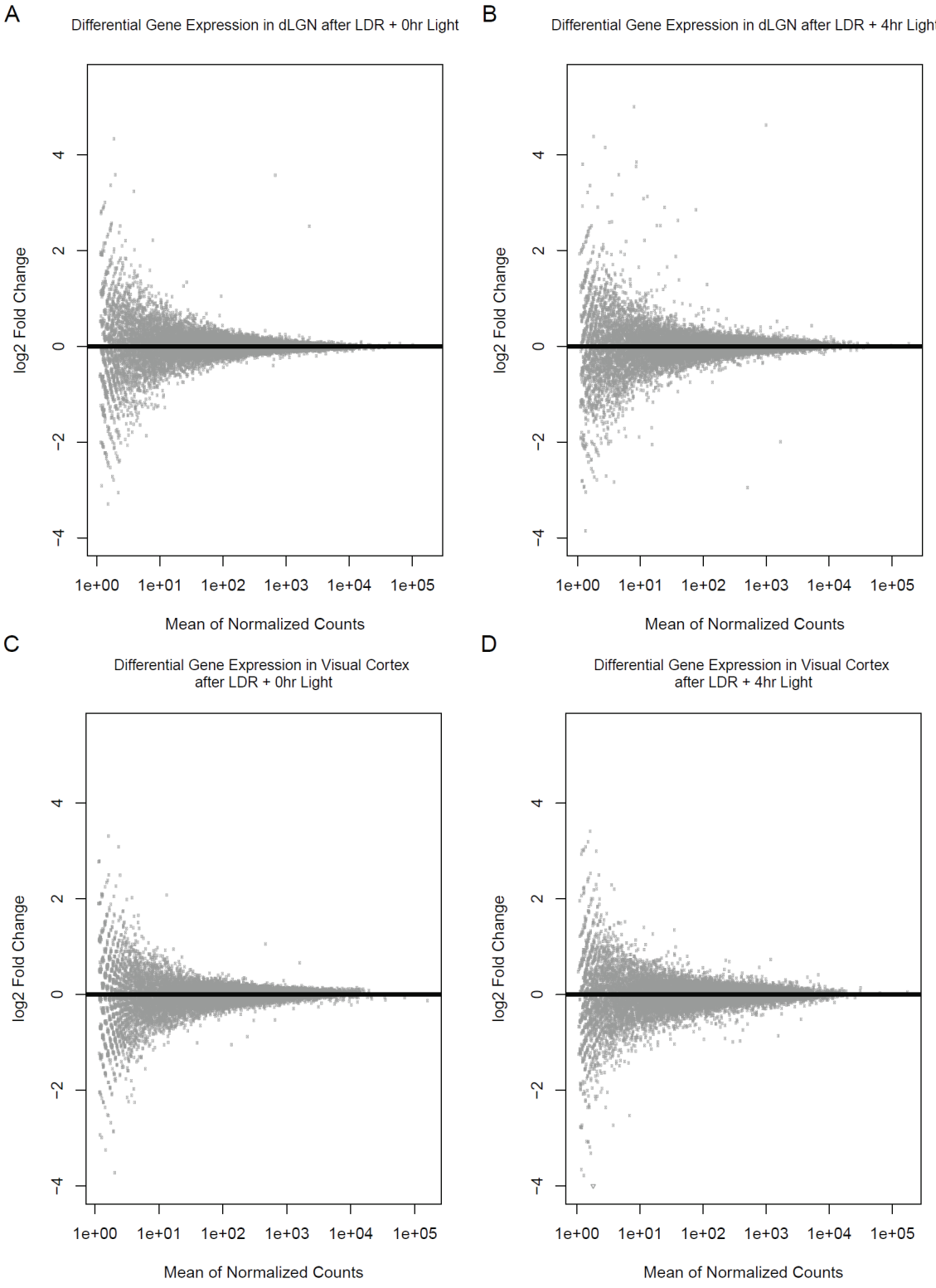

Figure S6. Late dark rearing (LDR) and light exposure did not reveal detectable activity-induced gene expression differences between wild-type and MeCP2 QKI mice.
A) Comparison of mean normalized counts versus $\log_2$ fold-changes for all genes between WT and QKI dLGN from mice after undergoing LDR and no light exposure reveals no significantly differentially expressed genes.
B) Comparison of mean normalized counts versus $\log_2$ fold-changes for all genes between WT and QKI dLGN from mice after undergoing LDR and 4 hours of light exposure reveals no significantly differentially expressed genes.
C) Comparison of mean normalized counts versus $\log_2$ fold-changes for all genes between WT and QKI visual cortices from mice after undergoing LDR and no light exposure reveals no significantly differentially expressed genes.
D) Comparison of mean normalized counts versus $\log_2$ fold-changes for all genes between WT and QKI visual cortices from mice after undergoing LDR and 4 hours of light exposure reveals no significantly differentially expressed genes.
n=4 for all conditions. $p > 0.05$, Wald test.

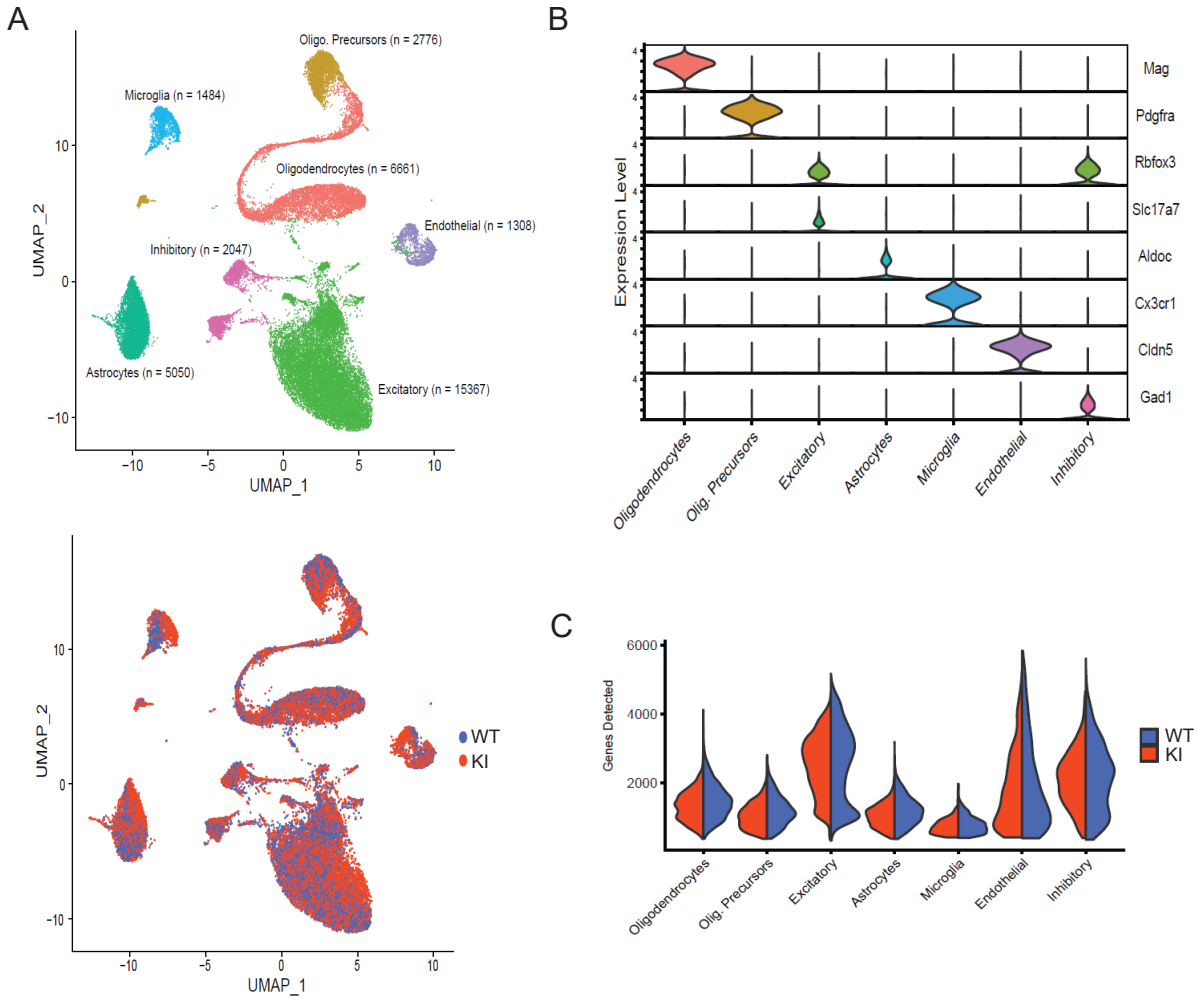

Figure S7. Single-nucleus RNA-seq analysis between WT and QKI mice.
A) UMAP visualization of WT and QKI snRNA-seq data from P20 dLGN revealed no differentially expressed genes between WT and QKI mice in excitatory neurons, inhibitory neurons, astrocytes, oligodendrocytes and oligodendrocyte precursors, or endothelial cells. One differentially expressed gene, *Atg16l2*, was detected in the microglia cluster. Three mice were pooled per genotype (n=2 replicates, 12 mice total). Cell types were assigned by known marker genes as discussed in Methods. Nuclei are colored by assigned cell type (*Top*) or by genotype (*Bottom*). n=number of nuclei per cluster. Oligo., oligodendrocyte.
B) Cell type assignment in P20 dLGN snRNA-seq dataset using the indicated marker genes. The y-axis indicates normalized counts.
C) Distribution of number of genes detected in nuclei in each cell type, by genotype. Blue, WT. Orange, QKI.

SUPPORTING METHODS

Phenotypic characterization of knock-in mice

Consistent with a previous study (1), mice were backcrossed a minimum of 3 generations before undergoing aging characterization and a minimum of 12 generations for behavioral scoring. For aging studies, WT (MeCP2-WT/Y) and QKI (MeCP2-QKI/Y) littermates were housed for a year, noting survival, which was graphed using Kaplan-Meier plots. Mice underwent phenotypic scoring, assessing mobility, gait, hindlimb clasping, tremor, breathing, and general condition, where mice akin to WT are scored 0, 1 with symptoms present, and 2 with severe symptoms as previously described (1). All assessments were performed blinded to genotype.

Electrophysiology

An Olympus BX51WI microscope with a 60x water immersion objective was used to identify TC neurons. Data acquisition was performed using Clampex10.2, an Axopatch 200B amplifier, and digitized with a DigiData 1440 data acquisition board (Molecular Devices, Sunnyvale, CA). Analysis of EPSCs was done using Clampfit (Molecular Devices, Sunnyvale, CA), Excel (Microsoft, Redmond, WA), Prism 9 (GraphPad Software, La Jolla, CA), and custom software written and generously shared by Dr. Bruce P. Bean in Igor Pro v6.1.2.1 (WaveMetrics, Lake Oswego, OR). For blinding of electrophysiology experiments, after tail or toe clippings were obtained from litters, C.P.T. prepared DNA, ran PCRs, and loaded 1 to 1.5% agarose gels for genotyping, after which L.D.B. imaged the gels and informed C.P.T. of the relevant mice to use for recordings by eartag number, without revealing whether such mice were WT or QKI. After recordings and analyses for a particular experiment were completed, L.D.B. revealed genotypes to C.P.T. for statistical analyses in GraphPad Prism 9.

Fiber Fraction

The fiber fraction (FF = single fiber current amplitude ÷ maximal current amplitude) was calculated to approximate RGC convergence onto each TC neuron in the dLGN. Maximal current amplitudes ("Max") were determined by stimulating the optic tract at increasing intensities ≥50 μA until the amplitude of the EPSC reached a plateau. Prior to recording EPSCs for each cell, a stimulating electrode filled with ACSF was moved along the optic tract in order to determine a site that would activate as many RGC axons as possible and yield the largest maximal EPSC current. A second electrode was positioned just above the surface of the slice to serve as a local ground. The stimulus intensity was then decreased systematically until a failure of synaptic transmission was observed, then increased by 0.25 μA until an EPSC was visible whose amplitude is the single fiber amplitude ("SF"). The fiber fraction is the SF amplitude divided by the maximal amplitude (FF = SF ÷ Max). For each stimulus intensity, we recorded the synaptic response at holding potentials of both −70 mV and +40 mV with an inter-trial interval of 20 seconds, yielding at least two fiber fraction values for each cell recorded. To determine NMDAR-mediated amplitudes, the more slowly rising peak NMDAR-mediated EPSCs were measured following the initial decay of the AMPAR transient. In some cases, only the minimal threshold response was quantified for SF amplitude because it was difficult to distinguish between the recruitment of an additional fiber from trial-to-trial variation of the same fiber.

However, if an incremental step in stimulation intensity of 0.25 μA recruited an EPSC with at least five times the amplitude of the initial SF EPSC at either −70 mV or +40 mV, this second SF amplitude was included in our analysis ("SF_2"). Our reasoning for this 5x cutoff is the inability to confidently attribute a modestly increased EPSC to the activation of a second RGC axon; we cannot exclude the possibility of stochastic variations in vesicular release of the initial SF. The 5x cutoff was determined after subtracting the first SF amplitude from the second SF amplitude. For "silent synapses", SF_2 was always included in our analysis regardless of amplitude because SF_1 at −70mV = 0. Additional details regarding the justification of fiber fractions are available in the supplementary sections of Hooks and Chen, 2008 and Noutel et al., 2011 (3, 4).

Eye-specific segregation in the LGN

QKI mice and littermate WT controls (P58-64) were anesthetized with isoflurane and injected intraocularly with 2 μL of a 2% solution of cholera toxin subunit B conjugated to Alexa Fluor 488 or Alexa Fluor 555. Four days after injection, mice were anesthetized with ketamine/xylazine and transcardially perfused with 4% paraformaldehyde. Coronal sections (75 μm) were mounted with mounting medium containing DAPI. Non-saturated 10x images were acquired with an Olympus DP72 camera on an Olympus BX63 fluorescent microscope. Images were analyzed using Fiji using a previously described threshold-independent method (4, 5). Background signal was subtracted and the

dorsal LGN was selected. The logarithm of the ratio of ipsilateral to contralateral channel intensity (R) was calculated for each pixel, and then the mean variance of R was calculated for each section. The mean variance of R was used to compare eye-specific segregation across genotypes.

Gene Expression from WT and MeCP2 T308A Mice

MeCP2 T308A mice and WT littermates were housed in the dark for 2 weeks starting at 6 weeks of age. At 8 weeks, mice were exposed to light for either 0 or 6 hours before visual cortex was dissected. RNA was purified as described in the Methods. For qPCR, cDNA was generated with the Superscript III First-Strand Synthesis System, and qPCR was performed with gene-specific primers (*below*) with SYBR green detection on a Roche Lightcycler 480. The expression of each target gene was normalized to the housekeeping gene Tubb3. RNA-seq was performed and analyzed as described in the Methods. *qPCR primers*:

Tubb3 F: CGACAATGAAGCCCTCTACGAC
Tubb3 R: ATGGTGGCAGACACAAGGTGGTTG
Bdnf F: GATGCCGCAAACATGTCTATGA
Bdnf R: TAATACTGTCACACACGCTCAGCTC
Arc F: TACCGTTAGCCCCTATGCCATC
Arc R: TGATATTGCTGAGCCTCAACTG
Npas4 F: ACCTAGCCCTACTGGACGTT
Npas4 R: CGGGGTGTAGCAGTCCATAC
Fos F: GGCAGAAGGGGCAAAGTAGA
Fos R: GCTGCAGCCATCTTATTCCG
Nptx2 F: CTTAGCCGCTCCTTGCAAAC
Nptx2 R: AGCCCAGCGTTAGACACATT

Late Dark Rearing

Vision-dependent gene expression was assessed by deprivation and subsequent synchronization of visual experience. Mice underwent dark rearing from P20-P27 (known as late dark rearing (LDR)) and were then acutely re-exposed to light for either 0 or 4 hours (6). Quantitative reverse transcription PCR (qRT-PCR) of RNA extracted from both visual cortex and dLGN was done to validate our stimulation protocol (*Figure S5*), using primers designed to anneal to the RNA transcripts of known activity-regulated genes, including the immediate early proto-oncogene *Fos* (7, 8), the bHLH-PAS transcription factor *Npas4* (9–11), brain-derived neurotrophic factor *Bdnf* (12–14), and the cytokine receptor *Tnfrsf12a* / *Fn14* (6):

Gapdh F: AGGTCGGTGTGAACGGATTTG
Gapdh R: GGGGTCGTTGATGGCAACA
Npas4 F: ACCTAGCCCTACTGGACGTT
Npas4 R: CGGGGTGTAGCAGTCCATAC
Fn14 F: GACCTCGACAAGTGCATGGACT
Fn14 R: CGCCAAAACCAGGACCAGACTA
Fos F: GGCAGAAGGGGCAAAGTAGA
Fos R: GCTGCAGCCATCTTATTCCG
Bdnf F: GATGCCGCAAACATGTCTATGA
Bdnf R: AATACTGTCACACACGCTCAGCTC

SnRNA-seq analysis

FASTQ files were created using the standard bcl2fastq pipeline from Illumina. Gene expression tables for each nuclear barcode were generated via the CellRanger 3.0.0 pipeline as designed by 10X Genomics. Samples were demultiplexed, and all QKI or WT samples were merged using the CellRanger aggr function using default parameters. The datasets were loaded into R and analyzed using the Seurat (v3) package. Nuclei were removed from the dataset if they contained fewer than 500 detected genes, displayed more than 5% of reads mapping to mitochondrial genes, or had RNA counts detected at a level greater than 2 standard deviations higher than the mean value in their assigned cell type (likely reflecting doublets and multiplets).

All nuclei in either QKI or WT samples were considered together for clustering and dimensionality reduction. Data was normalized using Seurat's (v3) NormalizeData, and the 2,000 top variable genes across nuclei were identified using FindVariableFeatures function. Data was integrated using FindIntegrationAnchors (16 dimensions) and IntegrateData (16 dimensions), and then scaled using ScaleData. Principal component analysis using the RunPCA function (npcs = 16) was then performed. A shared nearest neighbor graph was constructed using the FindNeighbors function (considering the top 16 principal components), and clustering was assigned using the FindClusters function (resolution = 0.5). After, clusters with fewer than 100 nuclei were removed.

The following marker genes were used to assign cell type clusters identified: pan-neuronal (*Rbfox3*); pan-excitatory neurons (*Slc17a7*); pan-inhibitory neurons (*Gad1*); oligodendrocytes (*Mag*); oligodendrocyte precursor cells (*Pdgfra*); astrocytes (*Aldoc*); microglia (*Cx3cr1*); endothelial cells (*Cldn5*). Differential gene expression analysis between

QKI and WT cells within each cluster was conducted using Wilcoxon Rank Sum test via the FindMarkers function (default parameters), and significant genes were defined as those with an adjusted p-value less than 0.05.

AUTHOR CONTRIBUTIONS

C.P.T., T.W., L.D.B, W.R., S.T., C.C., and M.E.G designed experiments. C.P.T. performed all electrophysiology experiments. C.P.T. (P30 & LDR), T.W. (P15, P16, & P20), L.D.B. (T308A), and K.M. performed all gene expression experiments. L.D.B., W.R., E.L., A.S., and R.S. generated the quadruple knock-in mouse, did initial characterization of QKI mice, and performed mass spectrometry experiments. S.T. performed eye-specific segregation experiments. C.L. performed RT-qPCR validation of the LDR and light exposure paradigm. C.P.T., T.W., L.D.B., E.C.G., C.C., and M.E.G. wrote the manuscript.

SUPPORTING REFERENCES

1. J. Guy, J. Gan, J. Selfridge, S. Cobb, A. Bird, Reversal of Neurological Defects in a Mouse Model of Rett Syndrome. *Science (80-.).* **315**, 1143–1147 (2007).
2. J. Guy, B. Hendrich, M. Holmes, J. E. Martin, A. Bird, A mouse Mecp2-null mutation causes neurological symptoms that mimic rett syndrome. *Nat. Genet.* **27**, 322–326 (2001).
3. B. M. Hooks, C. Chen, Vision triggers an experience-dependent sensitive period at the retinogeniculate synapse. *J. Neurosci.* **28**, 4807–4817 (2008).
4. J. Noutel, Y. K. Hong, B. Leu, E. Kang, C. Chen, Experience-Dependent Retinogeniculate Synapse Remodeling Is Abnormal in MeCP2-Deficient Mice. *Neuron* **70**, 35–42 (2011).
5. C. L. Torborg, M. B. Feller, Unbiased analysis of bulk axonal segregation patterns. *J. Neurosci. Methods* **135**, 17–26 (2004).
6. L. Cheadle, *et al.*, Visual Experience-Dependent Expression of Fn14 Is Required for Retinogeniculate Refinement. *Neuron* **99**, 525-539.e10 (2018).
7. M. E. Greenberg, E. B. Ziff, Stimulation of 3T3 cells induces transcription of the c-fos proto-oncogene. *Nature* **311**, 433–438 (1984).
8. E. L. Yap, *et al.*, Bidirectional perisomatic inhibitory plasticity of a Fos neuronal network. *Nature* **590**, 115–121 (2021).
9. Y. Lin, *et al.*, Activity-dependent regulation of inhibitory synapse development by Npas4. *Nature* **455**, 1198–1204 (2008).
10. B. L. Bloodgood, N. Sharma, H. A. Browne, A. Z. Trepman, M. E. Greenberg, The activity-dependent transcription factor NPAS4 regulates domain-specific inhibition. *Nature* **503**, 121–125 (2013).
11. I. Spiegel, *et al.*, Npas4 regulates excitatory-inhibitory balance within neural circuits through cell-type-specific gene programs. *Cell* **157**, 1216–1229 (2014).
12. P. B. Shieh, S. C. Hu, K. Bobb, T. Timmusk, A. Ghosh, Identification of a signaling pathway involved in calcium regulation of BDNF expression. *Neuron* **20**, 727–740 (1998).
13. X. Tao, S. Finkbeiner, D. B. Arnold, A. J. Shaywitz, M. E. Greenberg, Ca2+ influx regulates BDNF transcription by a CREB family transcription factor-dependent mechanism. *Neuron* **20**, 709–726 (1998).
14. E. J. Hong, A. E. McCord, M. E. Greenberg, A Biological Function for the Neuronal Activity-Dependent Component of Bdnf Transcription in the Development of Cortical Inhibition. *Neuron* **60**, 610–624 (2008).